WIND OBSERVATIONS OF SUPRATHERMAL ELECTRONS IN THE INTERPLANETARY MEDIUM

R. P. LIN
Space Sciences Laboratory and Physics Department, University of California, Berkeley, CA 94720–7300, U.S.A.

Abstract. We review some of the new results for suprathermal electrons obtained with the 3-D Plasma and Energetic Particle Instrument on the WIND spacecraft, which provides high sensitivity electron and ion measurements from solar wind thermal plasma up to $\gtrsim$MeV energies. These results include: (1) the observation of solar impulsive electron events extending down to $\sim$0.5 keV energy; (2) the observation of a turnover at $\sim$12 keV for electrons in a gradual large solar energetic particle (LSEP) event; (3) the detection of a quiet-time population (the 'superhalo') of electrons extending up to $\sim$100 keV energy; and (4) the probing of the magnetic topology and source region for magnetic clouds, using electrons. These unique WIND measurements are highly complementary to the particle composition measurements which will be made by ACE.

1. Introduction

For many years the solar wind thermal plasma has been regarded as a regime essentially independent from the energetic particle populations found in interplanetary space. Because of dynamic range considerations, previous instruments designed to measure the solar wind plasma ions and electrons lack the sensitivity to detect the suprathermal particles from just above solar wind plasma to a few hundred keV, except during highly disturbed times. These suprathermals play a key role in the varied plasma and energetic particle phenomena observed to occur in the interplanetary medium (IPM), and they provide information about their source, whether it is the Sun, the outer heliosphere, or the Earth.

The 3-D Plasma and Energetic Particles Experiment (Lin et al., 1995) on the WIND spacecraft is designed to bridge the gap between solar wind plasma and energetic particle measurements by providing high sensitivity, wide dynamic range, good energy and angular resolution, full 3-D coverage, and high time resolution over the energy range from a few eV to $\gtrsim$300 keV for electrons and $\gtrsim$6 MeV for ions. This is the only instrument operating during the Advanced Composition Explorer (ACE) mission that provides the sensitivity necessary to detect suprathermal electrons from just above the solar wind halo and strahl ($\lesssim$1 keV) to $\sim$30 keV. Observations in this range are essential for studies of particle acceleration at the Sun and in the IPM, for understanding wave-particle interactions in the IPM, and for probing the topology of large structures such as magnetic clouds. The mea-

Space Science Reviews **86:** 61–78, 1998.

surements of this instrument are thus highly complementary to those made by the instruments on the ACE mission.

2. Solar Impulsive Non-relativisitic Electron Events

The steady-state solar wind electron population is dominated by a core with temperature kT $\sim$10 eV, containing $\geq$95% of the plasma density and moving at about the solar wind bulk velocity, plus $\sim$5% in a hot, kT $\sim$80 eV, halo population carrying heat flux outward from the Sun, often in the form of a highly collimated strahl (Feldman et al., 1975). Impulsive non-relativistic electron events were first detected at energies above $\sim$40 keV (Van Allen and Krimigis, 1965; Anderson and Lin, 1966). However, the first high sensitivity measurements of electrons from $\sim$20 keV down to 2 keV, made by the ISEE-3 spacecraft, showed that impulsive acceleration of electrons occurred, on average, several times a day or more during solar maximum (Lin, 1985). Many of these non-relativistic electron events are unaccompanied by reported Hα flares, and many are observed only at energies below $\sim$15 keV.

Accelerated ions are detected above background for some of these electron events but the fluxes are generally very low, indicating the e/p ratio is large. The associated ion emission is primarily at low energies ($\sim$MeV nucl^{-1} and below) and ^{3}He-rich (Reames, von Rosenvinge, and Lin, 1985); that is, the ions have ^{3}He/^{4}He ratios of order unity while the typical ratios for the solar atmosphere or solar wind are a few times 10^{-4}. The soft X-ray (SXR) bursts accompanying these events are typically impulsive, with duration $\lesssim$10 min, so these non-relativistic electron-^{3}He-rich events are sometimes called impulsive solar energetic particle (SEP) events. As these electrons escape, they produce solar and interplanetary type III radio bursts through beam-plasma interactions (see Lin, 1990 for review). Table I, right column, summarizes the properties of these events.

Figure 1 shows a solar impulsive electron event observed by WIND (Lin et al., 1996) over the entire energy range from solar wind to suprathermal particle energies (a few eV to hundreds of keV). The main event beginning at 11:00 UT is easily identified by its velocity dispersion, i.e., the faster electrons arriving earlier, as expected if the electrons of all energies were simultaneously accelerated at the Sun and traveled the same distance along the interplanetary field to reach the spacecraft. The solar event can clearly be identified down to the 0.908 keV and even the 0.624 keV channels. A second, much weaker impulsive electron event is seen beginning about 16:20 UT in the 8.77 keV channel. Another very small event may be starting at $\sim$11:20 UT at $\sim$6 keV energy.

The 3-D angular distributions (Figure 2) show that the electrons in the main event are streaming outward from the Sun with pitch-angle distribution highly peaked, within $\lesssim$30°, along the magnetic field.

TABLE I
Solar energetic particle event characteristics

Characteristic	Large solar energetic particle (LSEP) events	Non-relativistic electron – ^{3}He-rich events
Dominant particle species	$\gtrsim$10 MeV protons	∼2–100 keV electrons
Electron to proton ratio	small	large
^{3}He/^{4}He ratio	'normal' solar ($\sim 5 \times 10^{-4}$)	∼0.1–1 (∼10^2 to $\gtrsim 10^3$ times normal)
Heavy nuclei	'normal' solar	enhanced abundances of Fe, Mg, Si, S
Ionization states	typical of 1–2 $\times$ 10^6 K normal corona e.g., Fe^{+13})	highly stripped (e.g., Fe^{+20}) typical of ∼10^7 K plasma
Extent in solar longitude	$\gtrsim$100 deg	tens of degrees
Event rate (at solar maximum)	tens per year	$\gtrsim 10^3$ per year
Flare association	large solar flare (but sometimes missing)	mostly small flares but often no flare
Solar soft X-ray burst	gradual, *e*-folding decay times >10 min	impulsive, e-folding decay times < 10 min
Interplanetary association	Coronal Mass Ejection (CME) with fast shock	interplanetary type III radio burst

Figure 3 shows electron differential flux vs energy spectra at different times during, and integrated over, the entire impulsive event, as well as the pre-event solar wind spectrum, with core, halo and 'super-halo' (discussed later). The event spectra have the pre-event spectra subtracted. The primary event spectra progress to lower energies with time; the peak in the spectrum at ∼5 keV at 12:30–12:40 UT moves to ∼3 keV at 13:00–13:10 UT and ∼2 keV at 14:00–14:10 UT. Contributions from the smaller events are also evident, e.g., at 11:45–11:55 UT. The event-integrated spectrum displays a peak at $\lesssim$1 keV, with significant flux at ∼0.5 keV. No electrons are detected in the 422 eV channel or below for this impulsive event. Above the peak, the spectrum is similar to those reported previously above ∼2 keV (Potter et al., 1980), and can be fit to a power-law shape $\mathrm{d}J/\mathrm{d}E = AE^{-\delta}$, where E is the electron energy in keV and A and δ are constants. The best fit gives $\delta = 3.0$ from ∼1 keV to 40 keV, steepening to $\delta = 4.4$ above ∼40 keV.

Because at coronal temperatures electrons are not gravitationally bound while protons are, an ambipolar electric field (the Pannekoek–Rosseland field (Pannekoek, 1922; Rosseland, 1924)) is set up with a total potential drop of about 1 kV from the base of the corona to 1 AU. This potential varies inversely with distance from Sun center, and it accelerates protons outward and decelerates electrons. Thus, the peak in the spectrum of the electrons just as they escape the corona could be up to

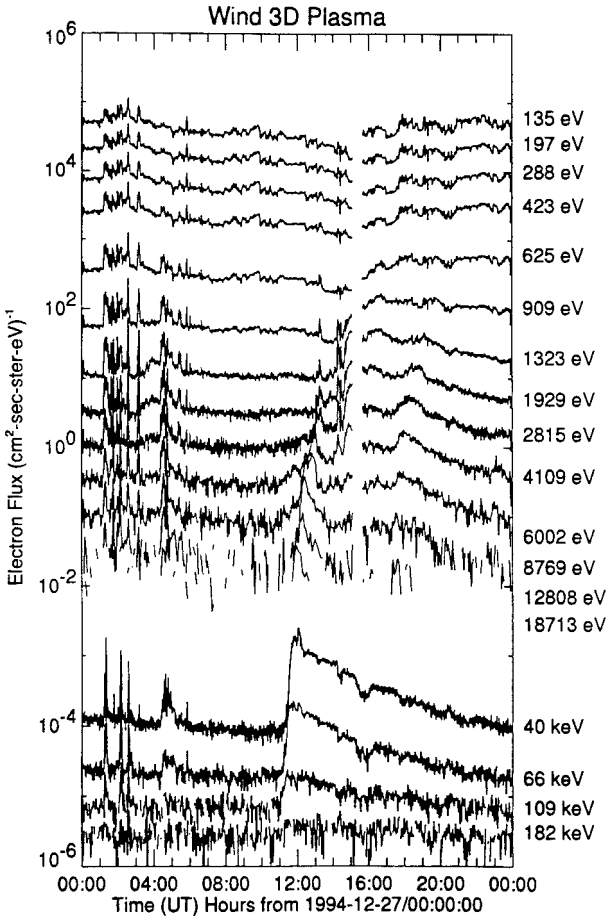

Figure 1. Electron fluxes from ∼100 eV to $\gtrsim$100 keV for 27 December 1994. The solar electron event begins at ∼11:00 UT at ∼100 keV, with velocity dispersion evident down to 624 eV. Two smaller events, at ∼11:00 UT and 16:20 UT, are visible below ∼6 keV. The dip at ∼15:00 UT at low energies is due to the close approach to the Moon, resulting in a plasma shadow (from Lin et al., 1996).

∼1 keV more than measured at 1 AU, e.g., ranging from $\lesssim$1 up to ∼2 keV for the event of Figure 1, depending on the height of the acceleration.

The fact that the event spectrum extends down to such low energies indicates that at least some of the electron acceleration must occur high in the corona, since the range of ∼keV energy electrons in ionized hydrogen, due to Coulomb collisions, is short compared to the column depth through the corona. Assuming that the initial accelerated electron spectrum is a power law with the same exponent as seen at energies above the peak, the maximum overlying column density can be calculated (Lin, 1974). For a peak at ∼1.5 keV, the column density must be less than $\sim 9 \times 10^{17}$ cm^{-2}. This value implies that the lowest energy electrons must

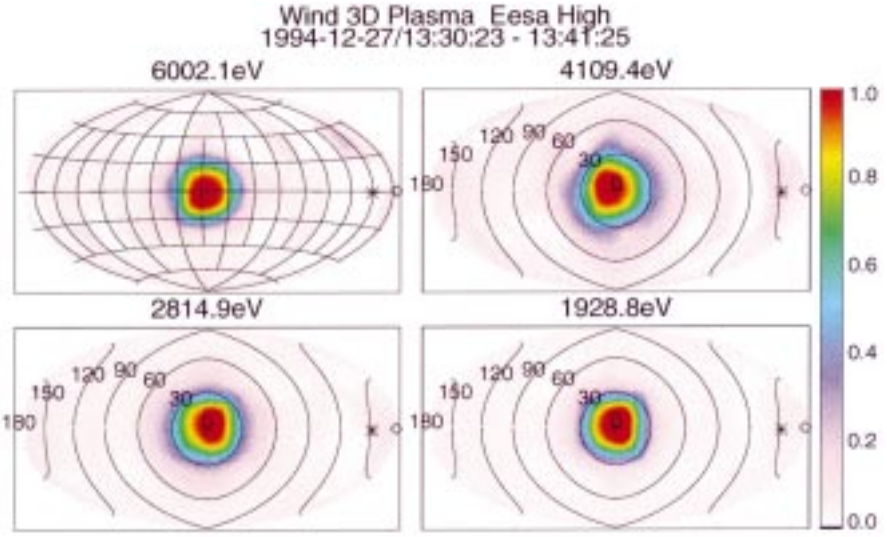

Figure 2. The 3-D angular distribution of the electrons during the impulsive event. the magnetic field direction is centered at the origin and the Sun direction indicated by the asterisk. The angular grid of the measurements (upper left panel) and pitch-angle contours are shown (from Lin et al., 1996).

have been accelerated at altitudes of $\sim$1 $R_\odot$, for the typical active coronal density models (Dulk and McLean, 1978), or $\sim$0.2 $R_\odot$ for the quiet equatorial corona at sunspot minimum (Saito et al., 1977).

A ^{3}He enhancement was detected in solar energetic ions during this electron event (J. Mazur, private communication, 1995). If the ^{3}He originated at the same altitude in the corona as these low energy electrons, the proposed mechanism of acceleration by electromagnetic hydrogen cyclotron waves (Temerin and Roth, 1992) would be ruled out since the magnetic field would be much too weak. However, a previous comparison of the solar flare X-ray spectrum with the escaping electron spectrum over the 2–100 keV energy range (Pan et al., 1983) for an event observed by ISEE-3 suggests that X-ray producing electrons are present over a region which extends from the chromosphere to the high corona, while the lowest energy escaping electrons come only from the high corona. Thus both the ^{3}He and the more energetic electrons might be accelerated in the lower corona where the magnetic field is higher.

Even though the first year of the WIND observation, late 1994 to late 1995, is near solar minimum, tens of impulsive solar electron events have been seen, with many detected down to $\sim$0.5 keV. The coronal flare acceleration process thus appears to produce a power-law spectrum extending down to $\lesssim$1.5 keV or lower, compared to a coronal thermal electron energy of kT $\sim$0.1 keV ($\sim 10^6$ K). Integrating over the energy spectrum and over the duration of the event, and assuming that the cone of propagation in the interplanetary medium for the electron event of Figure 4 is $\sim$40°, we estimate a total energy of $\gtrsim 3 \times 10^{26}$ ergs in escaping

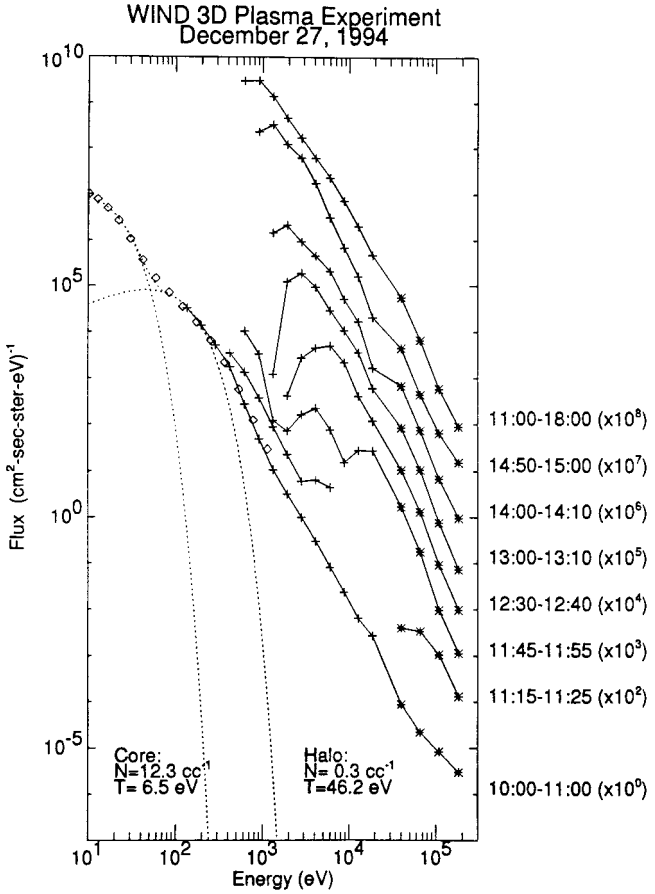

Figure 3. Omnidirectional electron spectra (with pre-event electron fluxes subtracted) are shown for various times during the 27 December 1994 event, and averaged over the entire event. The pre-event electron spectrum shows the solar wind electron core and halo components, as well as a 'super halo' extending to $\gtrsim$100 keV (from Lin et al., 1996).

electrons. Thus, at least that much energy was released in the coronal flare process at the Sun.

3. Large Solar Energetic Particle (LSEP) Events

The other type of solar energetic particle event (actually discovered first) produces significant flux of $>$10 MeV protons (Table I, left column). These are the largest (hence LSEP) and most energetic events. They usually occur after a large solar flare, and occasionally exhibit acceleration up to relativistic energies. Electrons are also observed, but the fluxes of energetic protons dominate over electrons. Tens of LSEP events are detected per year near solar maximum.

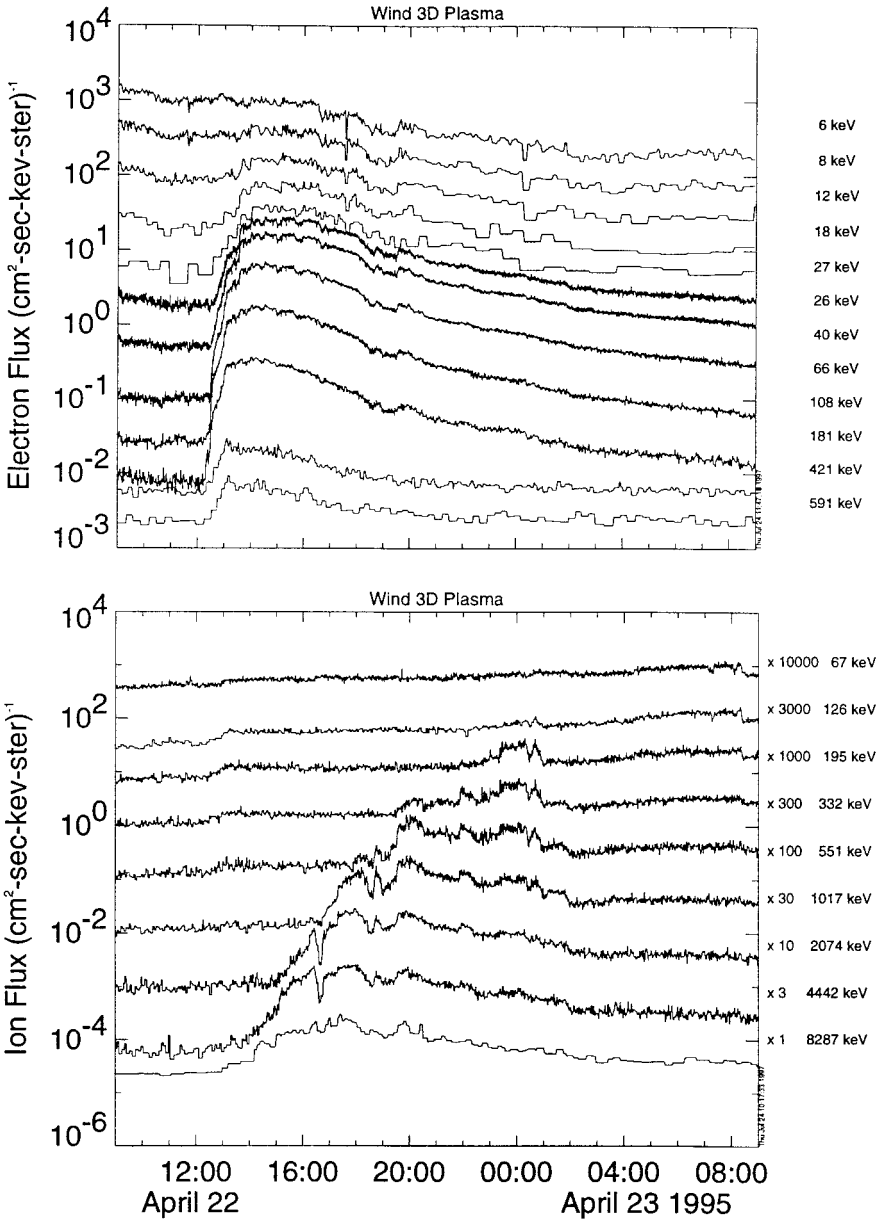

Figure 4. Energetic electron (*upper panel*) and ion (*lower panel*) fluxes for 22–23 April 1995. The energies (and flux factors) are indicated on the right. The gradual (LSEP) event is evident at energies above ∼12 keV in electrons.

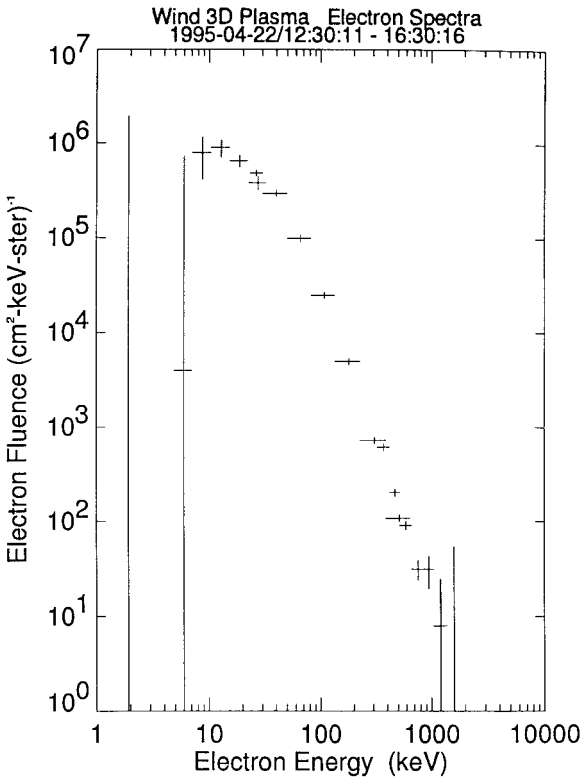

Figure 5. Omnidirectional electron energy spectrum (with pre-event background subtracted) averaged over the first four hours of the event.

The observed ionization states of LSEP particles are typical of a 1–2 $\times$ 10^6 K plasma, suggesting that these come from the quiescent solar corona and/or solar wind. It is believed that shock waves, from Coronal Mass Ejections (CME) or perhaps flares, propagating over a wide longitude range of the solar corona are the accelerating agent. LSEP events are also called 'gradual' events since they are typically accompanied by flare soft X-ray (SXR) emission of relatively long duration, with e-folding decay times of $\gtrsim$tens of minutes.

Figure 4 shows the 22 April 1995 SEP event, the first event observed by WIND where energetic solar ions up to $\gtrsim$20 MeV and electrons up to $\sim$1 MeV were detected. A M7.1 SXR burst with two maxima, a sharp impulsive spike at $\sim$11:50 UT and a second, much smaller, maximum at $\sim$12:30 UT followed by a gradual decay lasting several hours, was detected by GOES. The presence of significant fluxes of $>$10 MeV protons and the gradual SXR burst confirm this is an LSEP event, and no enrichment in ^{3}He was detected for this event (J. Mazur, private communication).

Electrons are detected down to $\sim$8 keV in this event (Figure 4), but no increase is detected below $\sim$6 keV, in contrast to the impulsive event of Figure 1. The electron spectrum for the event (Figure 5) shows a peak at $\sim$12 keV, and a rapid

falloff below ∼8 keV. Above ∼12 keV the spectrum fits a double power law with a break around 50 keV, and power-law exponents of $\delta = 1.1$ below and $\delta = 3.1$ above the break. If the peak is due to the electrons traversing overlying material, the source region is at a column depth of $\sim 1 \times 10^{19}$ cm^{-2}. Thus for quiet coronal density models the electrons would have been accelerated in the chromosphere, while for active corona models the height would be $\sim 0.15\ R_o$. In contrast, near solar maximum it was found that essentially all LSEP events with gradual SXRs have electron spectra extending down to 2 keV without turnover; the only events with a turnover were those with impulsive SXR bursts (Lin, 1990). The presence of this turnover at relatively high electron energies for this LSEP event suggests that the simple picture of particle acceleration by CME shocks high in the corona, or in the interplanetary medium, may need to be re-examined.

4. Quiet Time Electrons

Unlike ISEE-3, the WIND spacecraft was launched near the minimum in the solar activity cycle. Thus, there are substantial periods free from energetic solar particle events and streams. Figure 6 shows the WIND omnidirectional electron spectrum from ∼5 eV to ∼100 keV measured during such a quiet period on February 22, 1995. Because of the extremely wide range of electron fluxes, three separate detectors – EESA-L, EESA-H, and SST – are required to measure this spectrum. The Maxwellian core of the solar wind plasma dominates from ∼5 to ∼50 eV; the solar wind halo takes over from ∼100 eV to ∼1 keV. The halo is believed to be due to the escape of coronal thermal electrons which have a temperature of $\sim 10^6$ K. Note, however, that the halo spectrum departs significantly from isothermal at energies above ∼0.7 keV.

A third, much harder component has been discovered in the WIND observations, beginning above ∼2 keV and extends to $\gtrsim$100 keV, which we have denoted the ‘super-halo’. The spectrum of the ‘super-halo’ appears to be approximately power-law with exponent $\delta \sim 2.5$. If this ‘super-halo’ is solar in origin, it would imply that electrons of such energies must be continuously present at, and escaping from, the Sun.

The angular distribution of these ‘super-halo’ electrons at very quiet times appears to be nearly isotropic, however, with a very slight anisotropy flowing toward the Sun. Such angular distributions would be expected for sources beyond 1 AU; the near isotropy would be due to mirroring of this incoming population in the stronger magnetic fields of the inner heliosphere. Possibly, acceleration by Co-rotating Interaction Regions (CIRs) beyond 1 AU may be responsible for the superhalo, but a preliminary analysis shows no obvious one-to-one correlation with CIRs or with solar active regions.

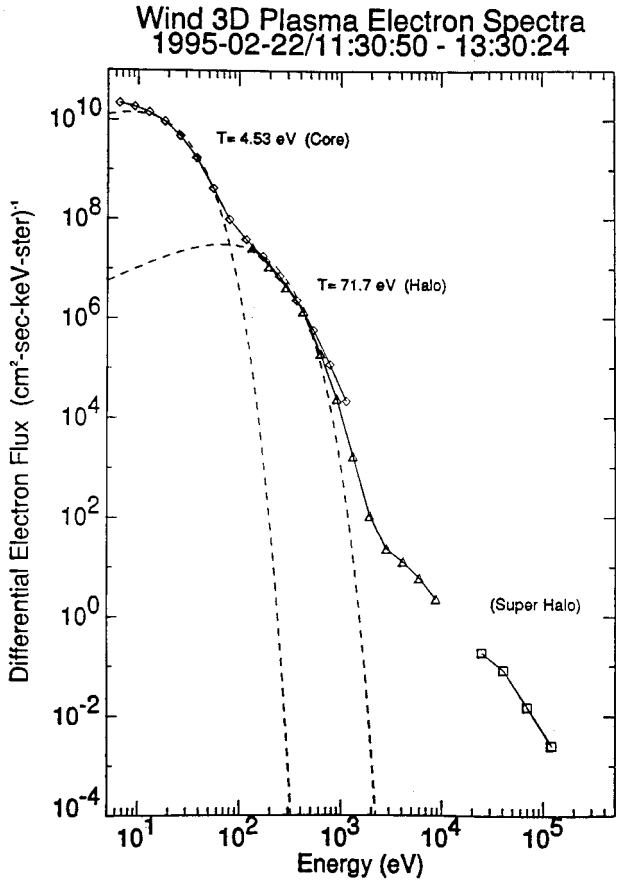

Figure 6. Electron differential flux spectrum from ∼5 eV to $\gtrsim$100 keV, measured at a very quiet time, in the absence of any solar particle events, by the WIND 3-D Plasma and Energetic Particle experiment. The diamonds, triangles, and squares indicate the three different detectors used to accommodate the wide range of fluxes over this energy range. The dashed lines give fits to Maxwellians for the solar wind core and halo.

5. Energetic Electrons, Plasma Waves, and Solar Type III Radio Bursts

Observations by the WIND 3DP instrument generally confirm the basic process for generating solar type III radio emission, wherein the velocity dispersion of the escaping electrons forms a beam which generates electron plasma (Langmuir) waves which in turn, produce electromagnetic (radio) emission (see Lin, 1990, for review).

Four solar impulsive electron events were detected by WIND on April 2, 1995 (Ergun et al., 1998). Figure 7(a) (top panel) plots the omnidirectional electron fluxes at 96s resolution as measured by EESAH. The center energies of the channels range from 140 eV to 27.1 keV, with the lowest energy traces on top. Immediately below (Figure 7(b)) are the omnidirectional electron fluxes as measured by the

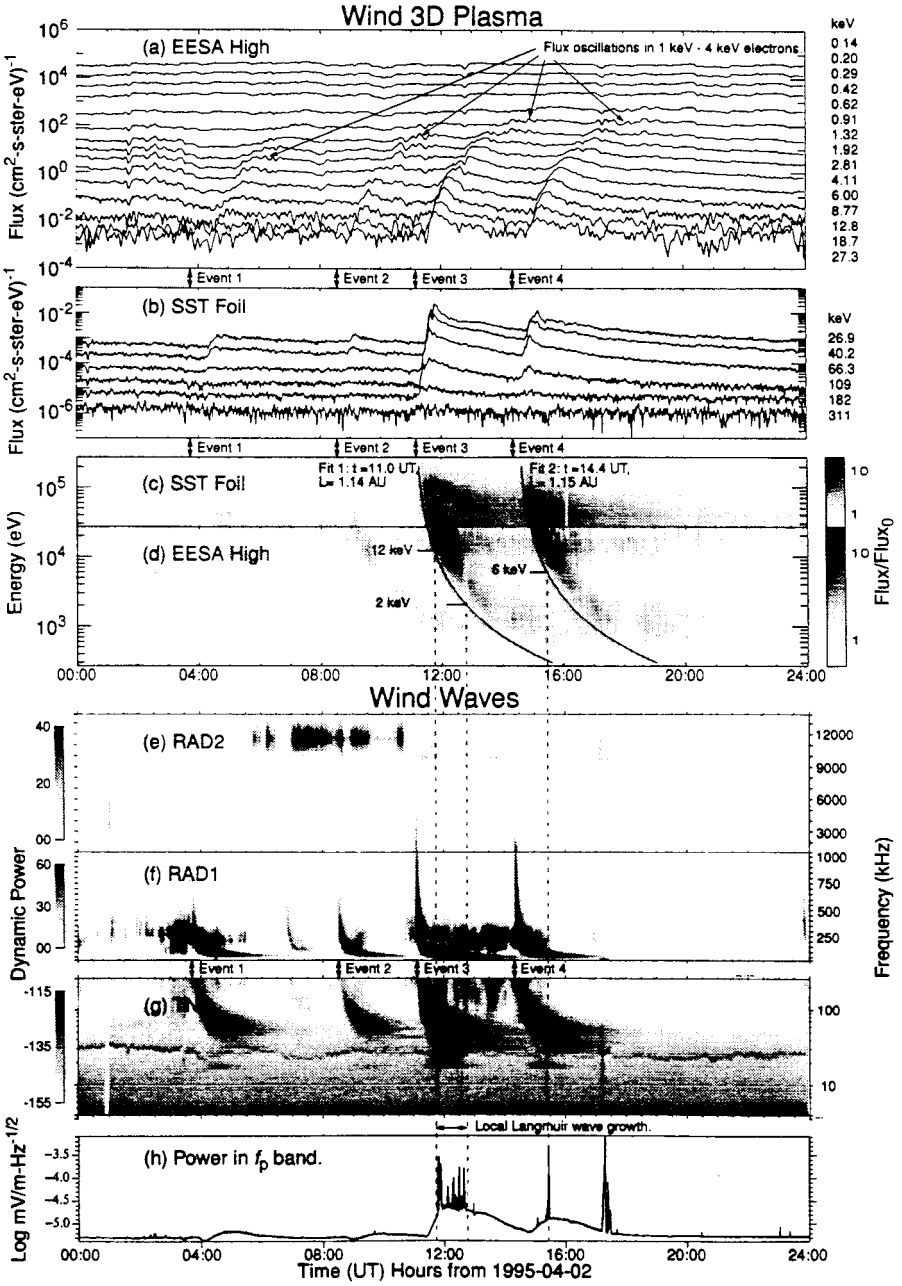

Figure 7. (a) The omnidirectional electron fluxes at 96s resolution as measured by EESA-H on WIND. The center energies are listed on the right. (b) The omnidirectional electron fluxes as measured by the SST- Foil detector. (c) and (d) Spectrograms of the ratio (F/F_0) of electron fluxes (F) to a reference flux (F_0) prior to the first event. Superimposed on the plot are linear fits of the arrival time of the electrons versus their inverse velocity. The event start times are marked on the plot. (e), (f), and (g) Solar type III radio bursts as observed by the WIND WAVES instrument. The RAD2 panel displays the radio emissions from 1 MHz to 14 MHz (linear frequency axis) The TNR (Thermal Noise Receiver) panel displays the frequency range from 4 kHz to 250 kHz. (h) The electric field wave power in the frequency band (19 kHz to 41.5 kHz) encompassing the local Langmuir frequency (from Ergun et al., 1998).

SST-Foil detector. The impulsive electron events can be clearly seen in the electron fluxes, with the strongest beginning at ∼11:10 UT with the 182 keV electrons and extending down in energy to ∼600 eV.

Persistent feature in all of the events were ∼15-min period modulations of the electron fluxes (see Figure 7(a)) that appeared as the low-energy (∼1 keV to ∼4 keV) electrons arrived. Similar flux modulations can be seen in several other solar impulsive electron events observed by the WIND satellite and by the ISEE-3 satellite (see Figure 3 of Lin et al., 1981). These modulations showed no measurable velocity dispersion, and the modulations of the second event are accompanied by modulations in the magnitude of the magnetic field with a similar period, suggesting some type of local hydromagnetic instability is occurring.

Figures 7(c) and 7(d) are spectrograms of the ratio (F/F_0) of the event electron fluxes (F) to the pre-event flux (F_0), determined by averaging from ∼00:00 UT to ∼04:00 UT. Superimposed on the spectrograms are linear fits of the arrival time of the electrons versus their inverse velocity. In all of the events, velocity dispersion of the electrons is consistent with the expected Archimedean spiral length (∼1.15 AU) for the measured solar wind velocity (∼370 km s^{-1}).

All four of the solar impulsive electron events were associated with solar type III radio bursts (Figure 7(e–g)) observed by the WIND WAVES instrument (Bougeret et al., 1995). The radio bursts for events 3 and 4 extended up to 14 MHz, the maximum frequency of the WAVES experiment. The lowest frequency radio electromagnetic emissions appeared to have a cut-off near the local second harmonic. The narrow-banded emissions that persisted throughout the day varying between 20 kHz and 40 kHz (see Figure 7(g)) are locally generated Langmuir waves; the power in Langmuir emissions is shown in Figure 7(h). The series of Langmuir bursts between ∼11:45 UT and ∼12:45 UT coincide with the arrival of ∼12 keV through ∼2 keV electron fluxes of event 3. The bursts at ∼15:25 UT coincided with the arrival of ∼6 keV electron fluxes of event 4.

Although the plasma processes involved in the generation of type III radio bursts are still not understood in detail (see Ergun et al., 1998), these observations confirm that the non-relavistic electrons are the source of the emission, and therefore the radio bursts can be used to track the escaping electrons from the Sun into the interplanetary medium.

6. Magnetic Clouds

Magnetic clouds are a type of CME characterized by relatively strong magnetic fields (low plasma beta) and a smooth rotation of the magnetic field direction over a ∼1 day period at 1 AU, consistent with the passage of an approximately force-free helical magnetic flux rope of diameter ∼0.25 AU (Burlaga, 1988). They often exhibit CME characteristics such as enriched alpha particle content, low proton temperature and bi-directional electron streaming (Gosling, 1996). The extended

periods of southward (and northward) magnetic field provided by the smooth rotation make clouds important for geomagnetic activity. As discussed by Gosling (1975) and MacQueen (1980) CMEs, including magnetic clouds, expel new magnetic flux, still connected to the Sun, into the interplanetary medium, so to maintain the IMF magnitude at a roughly constant level (King, 1979) compensating disconnection of magnetic flux must occur.

Larson et al. (1997) has shown that WIND electron observations of both the continuously outflowing halo at ∼0.1–1 keV and impulsive electron events from ∼1 to $\sim 10^2$ keV can be used to trace the magnetic field of a cloud back to the Sun, measure the lengths of the cloud field lines, and determine when magnetic disconnection from the Sun occurs.

The top three panels (a, b, c) of Figure 8 show the magnetic field strength ($|\mathbf{B}|$) and direction (Θ, Φ) for the October 18–20, 1995 magnetic cloud, from the magnetometer experiment on WIND (Lepping et al., 1995). Figures 8(d) and 8(e) show the solar wind speed and density respectively, measured by the 3DP experiment. A shock and magnetosheath-like region precede the cloud. The field rotates smoothly from south to north during the 30 hour passage of the cloud. Lepping et al. (1997) have fit this signature to a force-free flux-rope geometry and estimated the axis of the cloud to be nearly in the ecliptic plane ($\Theta = -12°$), close to the Parker spiral angle ($\Phi = 291°$), and with a right handed helicity. The cloud diameter is estimated to be about 0.27 AU and WIND passed very close to the central axis, ($y_0/R_0 = 0.087$).

Figure 8(f) shows the flux of electrons streaming away from the Sun (135°–180° pitch angles since $\Phi = 291°$) in 17 energy channels logarithmically spaced between ∼0.1 and 100 keV, respectively. At energies $\gtrsim$20 keV, several impulsive electron events with rapid rise and slow decay can be seen, for example, at ∼21:00 UT October 18, ∼06:00, ∼11:30 and ∼18:00 UT October 19. These events are also evident at lower electron energies, and generally show velocity dispersion.

Figure 8(g) shows a color spectrogram of the ratio F/F_0 of the outward streaming electron flux, F (pitch angles 135°–180°) divided by an average background flux (F_0) in the absence of impulsive events, to illustrate the velocity dispersion in the arrival of energetic electrons impulsively accelerated at the Sun. Figure 8h is a color spectrogram of the radio observations provided by the WAVES instrument on WIND. The numerous fast drift bursts, from high (14 MHz) to low (tens of kHz) frequency, are solar type III radio bursts. produced by fast electrons propagating from near the Sun (a few solar radii) to ∼1 AU, as discussed in the preceding section.

Each of the impulsive electron events can be traced back, with the type III radio burst produced by these electrons, to a flare observed by the *Yohkoh* Soft X-ray Telescope within solar active region 7912. Clearly, electrons accelerated in these flares escape outward along open field lines and are detected by the 3-D Plasma experiment if the WIND spacecraft is on a field line connected to the flare site. This tracking by the type III radio bursts of these electron events from ∼1 AU back

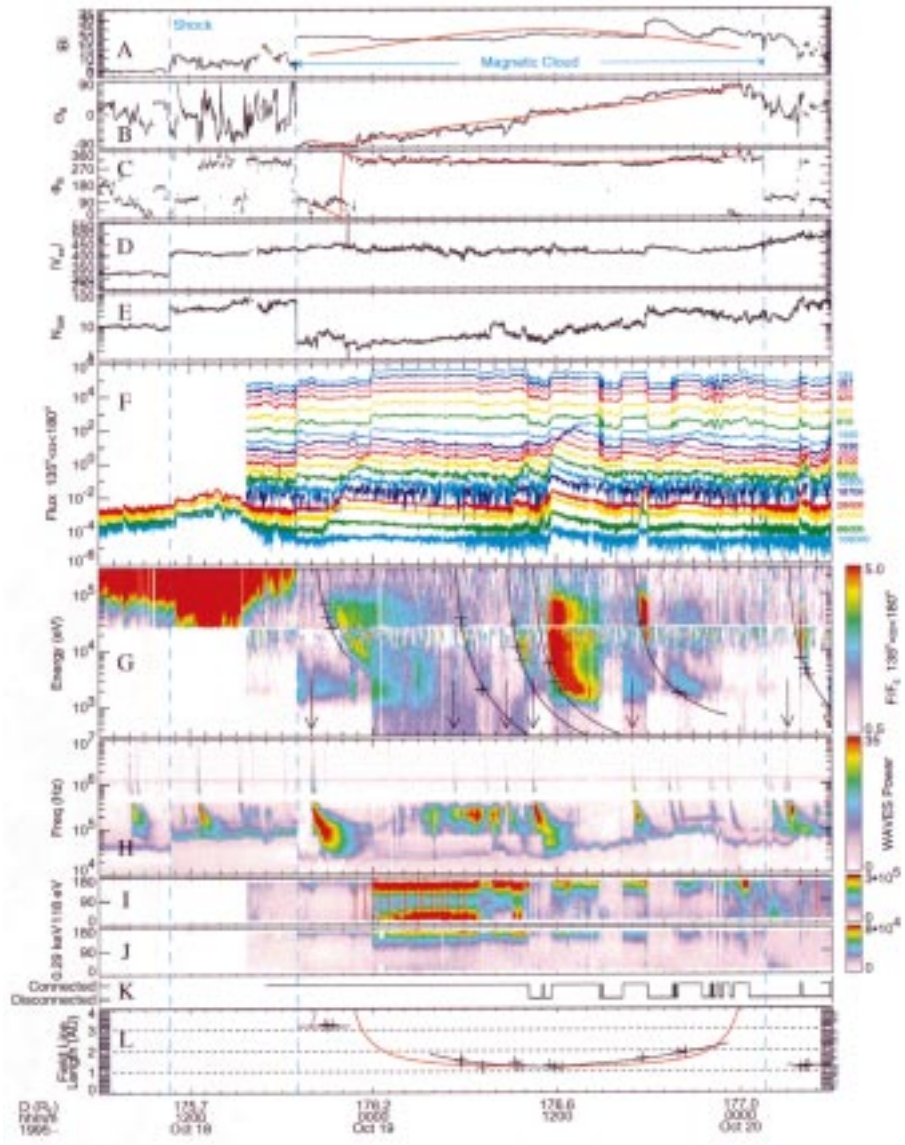

Figure 8. Summary plot of cloud event showing the magnetic field magnitude ($|B|$) and direction (Θ, Φ) in panels (A), (B) and (C). Solar wind speed and density are shown in panels (D) and (E). Panel (F) shows the electron flux for electrons traveling anti-parallel ($135° < a < 180°$) to the magnetic field direction for 18 logarithmically-spaced energy channels ranging in energy from ~0.14 to 110 keV. The following spectrogram (G), presents the ratio, F/F_0, of electron flux (F) divided by an average background flux (F_0) measured in the absence of impulsive solar electron events. Panel (H) is a spectrogram of the radio observations from 10 kHz to 10 MHz from the WIND WAVES experiment. Panels (I) and (J) are pitch-angle spectrograms of electrons at 118 eV and 290 eV. Magnetic connection to, or disconnection from, the Sun along the negative leg of the cloud is indicated in (K). From the flare time (arrows, (G)) and the arrival time of electrons as a function of energy, the field line length at each point was determined and is shown in panel (L). The black curve in panel (L) is a smooth curve drawn by hand. The red curves in panels (A), (B), (C) and (I) show the expected values for a model flux rope.

to X-ray flares at the Sun provides the first direct identification of the footprints of the magnetic fields of a cloud, in this case to an active region.

The crosses in Figure 8(g) mark the initial onset (at various energies) of the injected electrons. Using the start of the solar type III burst – identified by the sharp increase in >5 MHz wave power measured by the WAVES experiment – as the electron injection time (arrows) at the Sun, the field line length $L = v_e \Delta_t$ traveled by the electrons was determined and plotted in Figure 8(l). The field line length varies from ∼3 AU near the leading edge of the cloud to ∼1.2 AU near the center and rises again on the trailing part, qualitatively consistent with a flux rope model (smooth curve drawn in Figure 8(l)) with field lines twisted about a central core. The 3 AU outer field line compared to ∼1.2 AU near to the axis implies that it undergoes ∼4 turns from the Sun to 1 AU, or ∼8 turns for the entire cloud, assuming symmetry. The number of turns should be invariant if the field has not been magnetically reconnected while propagating from the Sun to 1 AU. The implication is that the flux rope was highly coiled at the time of ejection from the Sun.

Figures 8(i) and 8(j) show pitch-angle spectrograms of 118 eV and 289 eV halo electrons. Early in the cloud (∼19:00 UT October 18–07:00 UT October 19), bi-directional streaming of halo electrons is observed, indicating that both ends of the cloud field line are connected back to the solar corona. Later, after ∼07:00 UT October 19, the electron pitch-angle distributions are uni-directional, indicating magnetic connection to the Sun on only one leg of the cloud. In addition, the electron fluxes exhibit many abrupt, discontinuous drops in level, occurring simultaneously at all energies (see Figure 8(f)).

The pitch-angle spectrograms of Figures 8(i) and 8(j) identify these as heat flux dropouts (HFDs), which McComas et al. (1989) suggested are due to the disconnection of the IMF from the corona. Almost all the HFDs for this cloud extend up to high energies, and are observed in the impulsive events as well, confirming that these are times when the magnetic field is truly completely disconnected from the Sun, unlike many of McComas et al.'s HFDs which were not dropouts above 2 keV (Lin and Kahler, 1992). Figure 8(k) plots the connection to the Sun. Note that the disconnected regions range from a few minutes to hours long and they are intertwined with connected regions.

As the magnetic cloud passes by, the spacecraft crosses field lines with different connectivity (Figure 8(K)). The disconnections presumably result from magnetic reconnection near the Sun. Since the HFDs are observed simultaneously across all electron energies, the disconnections must have occurred >6 hours earlier (the travel time to 1 AU for the slowest electrons). Furthermore, the flux of energetic (20 keV/nuclon) ions (from the Energetic Particle: Acceleration Composition and Transportation (EPACT) investigation on WIND (von Rosenvinge et al., 1995)) shows coincident dropouts, implying the disconnections occurred as much as ∼20 hours before the HFDs are detected at 1 AU.

Burlaga (1991) and Rust (1994) suggest that magnetic clouds are the interplanetary manifestation of solar filaments (prominences on the limb), which are often observed to have helical magnetic topology and to be embedded in CMEs. Gosling et al. (1995) have argued that magnetic clouds are formed by 3-dimensional reconnection of sheared magnetic arcades, and that, in the process, a mix of field lines connected at one end, at both ends and completely disconnected from the Sun can be produced. Alternatively, the cloud could also have emerged from the solar surface and been ejected from the Sun as a fully evolved flux rope with little or no reconnection.

We believe the disconnections probably occurred after the ejection of the cloud from the Sun ∼4 days earlier; otherwise the magnetic tension forces might be expected to significantly distort the cloud. As the cloud moves through the interplanetary medium, the legs of the flux rope may become partially disconnected from the solar surface through magnetic reconnection with adjacent field lines. Evidence for this is provided by an interplanetary type III radio storm detected by the WIND WAVES experiment in the 2.0–5.0 MHz range following the ejection of the cloud and prior to its detection at 1 AU. Such storms are believed to be the results of magnetic reconnection of magnetic fields high (∼1 R_s) in the solar corona (Bougeret et al., 1984).

7. Summary

The unique measurements of ∼1–30 keV suprathermal electrons provided by the WIND 3-D Plasma and Energetic Particle experiment are highly complementary to the energetic particle composition measurements which will be made from ACE. Together with solar observations from SOHO, Yohkoh, and TRACE, these observations will enable comprehensive studies of the origin of solar energetic particles and the tracing of interplanetary structures back to the Sun.

Acknowledgements

This research was supported in part by NASA grant NAG5–2815.

References

Anderson, K. A. and Lin, R. P.: 1966, 'Observations on the Propagation of Solar Flare Electrons in Interplanetary Space', *Phys. Rev. Letters* **16**, 1121.

Bougeret, J.-L., Kaiser, M. L., Kellogg, P. J., Manning, R., Goetz, K., Monson, S. J., Monge, N., Friel, L., Meetre, C. A., Perche, C., Sitruk, L., and Hoang, S.: 1995, 'WAVES: the Radio and Plasma Wave Investigation on the WIND Spacecraft', *Space Sci. Rev.* **71**, 231.

Bougeret, J.-L., Fainberg, J., and Stone, R. G.: 1984, 'Interplanetary Radio Storms', *Astron. Astrophys.* **141**, 17.

Burlaga, L. F.: 1988, 'Magnetic Clouds and Force-Free Fields with Constant Alpha', *J. Geophys. Res.* **93**, 7217.

Burlaga, L. F.: 1991, 'Magnetic Clouds', in R. Schwenn and E. Marsch (eds), *Physics of the Inner Heliosphere II*, Springer-Verlag, Berlin, p. 1.

Dulk, G. A. and McLean, D. J.: 1978, 'Coronal magnetic fields', *Solar Phys.*, **57**, 279.

Ergun, R. E., Larson, D., Lin, R. P., McFadden, J. P., Carlson, C. W., Anderson, K. A., Muschietti, L., McCarthy, M., Parks, G., Rème, H., Bosqued, J. M., d'Uston, C., Sanderson, T. R., Wenzel, K. P., Kaiser, M., Lepping, R. P., Bale, S. D., Kellogg, P., and Bougeret, J. L.: 1998, 'Wind Spacecraft Observations of Solar Impulsive Electron Events Associated with Solar Type III Radio Bursts', *Astrophys. J.* **503**, 435.

Feldman, W. C., Asbridge, J. R., Bame, S. J., Montgomery, M. D., and Gary, S. P.: 1975, 'Solar Wind Electrons', *J. Geophys. Res.* **80**, 4181.

Gosling, J. T.: 1975, 'Large-Scale Inhomogeneities in the Solar Wind of Solar Origin', *Rev. Geophys.* **13**, 1053.

Gosling, J. T., Birn, J., and Hesse, M.: 1995, 'Three-Dimensional Magnetic Reconnection and the Magnetic Topology of Coronal Mass Ejection Events', *Geophys. Res. Letters* **22** (8), 869.

Gosling, J. T.: 1996, 'Corotating and Transient Solar Wind Flows in Three Dimensions', *Ann. Rev. Astron. Astrophys.* **34**, 35.

King, J. H.: 1979, 'Solar Cycle Variations in IMF Intensity', *J. Geophys. Res.* **84**, 5938.

Larson, D. E., Lin, R. P., McTiernan, J. M., McFadden, J. P., Ergun, R. E., McCarthy, M., Rème, H., Sanderson, T. R., Kaiser, M., Lepping, R. P., and Mazur, J.: 1997, 'Tracing the Topology of the October 18–20, 1995 Magnetic Cloud with $\sim$0.1–10^2 keV Electrons', *Geophys. Res. Letters* **24**, 1911.

Lepping, R. P., Acuna, M. H., Burlaga, L. F., Farrell, W. M. et al.: 1995, 'The WIND Magnetic Field Investigation', *Space Sci. Rev.* **71**, 207.

Lepping, R. P., Burlaga, L. F., Szabo, A., Ogilvie, K. W., Mish, W. H., Vassiliadis, D., Lazarus, A. J., Steinberg, J. T., Farrugia, C. J., Janoo, L., and Mariani, F.: 1997, 'The WIND Magnetic Cloud and Events of October 18–20, 1995: Interplanetary Properties and as Triggers for Geomagnetic Activity', *J. Geophys. Res.* **102**, 14049.

Lin, R. P.: 1974, 'Non-Relativstic Solar Electrons', *Space Sci. Rev.* **16**, 189.

Lin, R. P.: 1985, 'Energetic Solar Electrons in the Interplanetary Medium', *Solar Phys.* **100**, 537.

Lin, R. P.: 1990, in E. Priest and V. Krishan (eds), 'Electron Beams and Langmuir Turbulence in Solar Type III Radio Bursts Observed in the Interplanetary Medium', *Basic Plasma Processes on the Sun*, International Astronomical Union, The Netherlands, p. 467.

Lin, R. P. and Kahler, S. W.: 1992, 'Interplanetary Magnetic Field Connection to the Sun During Electron Hear Flux Dropouts in the Solar Wind', *J. Geophys. Res.* **97**, 8203.

Lin, R. P., Potter, D. W., Gurnett, D. A., and Scarf, F. L.: 1981, 'Energetic Electrons and Plasma Waves Associated witha Solar Type III Radio Burst', *Astrophys. J.* **251**, 364.

Lin, R. P., Anderson, K. A., Ashford, S., Carlson, C., Curtis, D., Ergun, R., Larson, D., McFadden, J., McCarthy, M., Parks, G. K., Rème, H., Bosqued, J. M., Coutelier, J., Cotin, F., d'Uston, C., Wenzel, K.-P., Sanderson, T. R., Henrion, J., and Ronnet, J. C.: 1995, 'A Three-Dimensional Plasma and Energetic Particle Investigation for the Wind Spacecraft', *Space Sci. Rev.* **71**, 125.

Lin, R. P., Larson, D., McFadden, J., Carlson, C. W., Ergun, E. R., Anderson, K. A., Ashford, S., McCarthy, M., Parks, G. K., Rème, H., Bosqued, J. M., d'Uston, C., Sanderson, T. R., Wenzel, K.-P.: 1996, 'Observation of an Impulsive Solar Electron Event Extending Down to ∼0.5 keV Energy', *Geophys. Res. Letters* **23**, 1211.

MacQueen, R. M.: 1980, 'Coronal Transients: A Summary', *Phil. Trans. R. Soc. London, Ser.* **A297**, 605.

McComas, D. J., Gosling, J. T., Philips, J. L., Bame, S. J., Luhmann, J. G., and Smith, E. J.: 1989, 'Electron Heat Flux Dropouts in the Solar Wind: Evidence for Interplanetary Magnetic Field Reconnection?', *J. Geophys. Res.* **94**, 6907.

Pan, L., Lin, R. P., and Kane, S. R.: 1983, 'Comparisons of Solar Flare X- Ray Producing and Escaping Electrons from ∼2 to 100 keV', *Solar Phys.* **91**, 345.

Pannekoek, A.: 1922, 'Ionization in Stellar Atmospheres', *Bull. Astron. Inst. Neth.* **1**, 107.

Potter, D. W., Lin, R. P., and Anderson, K. A.: 1980, 'Impulsive 2–10 keV Solar Electron Events Not Associated with Flares', *Astrophys. J.* **236**, L97.

Reames, D. V., von Rosenvinge, T. T., and Lin, R. P.: 1985, 'Solar ^{3}He-Rich Events and Nonrelativistic Electron Events: A New Association', *Astrophys. J.* **292**, 716.

Rosseland, S.: 1924, 'Electrical State of a Star', *Monthly Notices Roy. Astron. Soc.* **84**, 720.

Rust, D. W.: 1994, 'Spawning and Shedding Helical Magnetic Fields in the Solar Atmosphere', *Geophys. Res. Letters* **21**, 241.

Saito, K., Poland, A. I., and Munro, R. H.: 1977, 'A Study of the Background Corona Near Solar Minimum', *Solar Phys.* **55**, 121.

Temerin, M. and Roth, I: 1992, 'The Production of ^{3}He and Heavy Ion Enrichments in ^{3}He-Rich Flares by Electromagnetic Hydrogen Cyclotron Waves', *Astrophys. J.* **391**, L105.

Van Allen, J. A. and Krimigis, S. M.: 1965, 'Impulsive Emission of ∼40 keV Electrons from the Sun', *J. Geophys. Res.* **70**, 5737.

Von Rosenvinge, T. T., Barbier, L. M., Karsch, J., Liberman, R. et al.: 1995, 'The Energetic Particles: Acceleration, Composition, and Transport (EPACT) Investigation on the Wind Spacecraft', *Space Sci. Rev.* **71**, 155.